The following manuscript was accepted for publication in Pharmaceutical Sciences. It is assigned to an issue after technical editing, formatting for publication and author proofing.
Citation: Safari F, Mirzaeei S, Mohammadi G. Development of Chitosan–Tripolyphosphate Nanoparticles as Glycopeptide Antibiotic Reservoirs and Ex vivo Evaluation for Their Potential to Enhance the Corneal Permeation in Ocular Drug Delivery. Pharm Sci. 2021, doi:10.34172/PS.2021.62

Development of Chitosan–Tripolyphosphate Nanoparticles as Glycopeptide Antibiotic Reservoirs and *Ex vivo* Evaluation for Their Potential to Enhance the Corneal Permeation in Ocular Drug Delivery

Farhad Safari[1], Shahla Mirzaeei [2,3*], Ghobad Mohammadi[2,3]

[1]Student Research Committee School of Pharmacy, Kermanshah University of Medical Sciences, Kermanshah, Iran

[2]Nano Drug Delivery Research Center, Health Technology Institute, Kermanshah University of Medical Sciences, Kermanshah, Iran

[3]Pharmaceutical Sciences Research Center, Health Institute, Kermanshah University of Medical Sciences, Kermanshah, Iran

***Correspondence:** Shahla Mirzaeei. Nano Drug Delivery Research Center, Health Technology Institute, Kermanshah University of Medical Sciences, Kermanshah, Iran. E-mail: shahlamirzaeei@gmail.com.

Address: Kermanshah University of Medical Sciences, Kermanshah, Iran. Tel.: +98-8334276489

Abstract

Purpose: The present investigation aimed to prepare Vancomycin-loaded nanoparticles (VAN-NPs) using chitosan (CS) and tripolyphosphate (TPP) besides exploring the effects of changing CS/TPP ratio on the physicochemical properties, corneal permeation, and ocular delivery of the prepared NPs.

Methods: Different pre-formulations were prepared using the modified ionic gelation process, then were characterized in terms of size distribution. Optimized formulations were furtherly evaluated by some characteristic tools such as Fourier-transform infrared (FTIR) spectroscopy and thermogravimetric analysis (TGA). The *in vitro* antimicrobial efficacy and drug release amounts along with the *Ex-vivo* corneal permeation of NPs through the sheep cornea were investigated. Quantification was performed using High-Performance Liquid Chromatography.

Results: Spherical and uniformly distributed NPs were developed with a mean particle size varied between 215–290 nm. FTIR spectroscopy confirmed that the CS/TPP cross-linking has taken place without affecting the pharmacologically active moiety of the drug. The obtained zeta potential values were in the range of +34 to +37 mV, which could ensure the stability of formulations. TGA analysis indicated enhanced thermal stability for the encapsulated drug compared to the plain drug. Formulations indicated suitable antimicrobial efficacy while releasing more than 90% of the drug during 24 h. NPs offered a 10-fold enhancement in corneal permeation compared to the drug solution.

Conclusions: Although further *in vivo* evaluation is still required to completely confirm the efficacy of the formulations, the enhanced release and corneal permeation of the drug suggest that the prepared NPs are suitable for ocular delivery of VAN.

Keywords: Antibiotic, Chitosan, Corneal permeation, Nanoparticles, Ocular drug delivery, Vancomycin.

1. Introductions

Ocular drug delivery has always been a major challenge for scientists due to the specific anatomy and structure of the eye as one of the most complex organs in the human body.[1,2] Despite being the most popular preparations, conventional topical drug delivery systems face some obstacles such as limited bioavailability and therapeutic efficacy come across with different defensive mechanisms including the almost impermeable nature of the eye, the natural reflex of blinking, and the tear film turnover.[3,4] Novel drug delivery systems can improve drug delivery by prolonging the corneal contact time and increasing the permeation of the drug into the eyeball.[5] To date, different formulations including liposomes, nanoparticles, nanofibers, nanoemulsions, etc. have been designed and developed mostly utilizing nanotechnology to improve the ocular delivery of various drugs.[6-9]

Corneal permeability is an effective factor in the determination of the therapeutic efficacy of topical preparations. Many drugs need to pass through the cornea to arrive at their site of action for a therapeutical effect. External agents can take two paths in order to permeate deeper into the cornea including transcellular and paracellular pathways. Both abovementioned pathways are usually blocked by the special arrangement of cells and layers against the passage of different drugs. Eventually, less than 10% of the administrated drug will permeate through the cornea.[10] Therefore, to achieve the desired concentration of drug at the posterior segment of the eye, either the injectable forms or the permeation enhancers should be used. Injectable forms are invasive and non-compliant; hence, physical enhancers and novel delivery systems are the foremost choices.[11]

Nanoparticles (NPs) are colloidal delivery systems with unique properties that made them suitable for targeted drug delivery.[12,13] Polymeric NPs can enhance ocular drug delivery owing to many

beneficial characteristics. These systems have the advantages of non-irritancy, increased residence time, and enhanced permeation through the cornea owing to the small particle size, positively charged surface, mucoadhesive nature, and a higher surface area.[14,15]

Chitosan (CS) is a natural biodegradable polymer with a wide variety of benefits like non-toxicity, mucoadhesive properties, and a high positive charge which make it one of the most promising agents for the preparation of ocular drug delivery enhancers.[16-18] Sialic acid residue of mucin layer contributes to creating a negative charge on the surface of corneal cells.[19-21] High affinity of CS-based NPs with a positive charge to this negatively charged corneal epithelium, eventually leads to a prolonged release of the drug. Furthermore, CS-based NPs exert potential antibacterial activity by interacting with the cell membrane of bacteria which can facilitate the therapeutic activity of antibiotic-loaded NPs.[22]

Vancomycin (VAN) is a glycopeptide antibiotic specifically used against methicillin-resistant Staphylococcus aureus (MRSA) infections which have a great role in endophthalmitis. The intravenous administration of this drug had the limitations of not achieving the desired concentration at the ocular tissues, besides being invasive, and non-self-administrable. As a result, recently, attempts have been made to develop topical ocular delivery systems of VAN which could overcome the discussed challenges and limitations.[23]

The present study aimed to design and develop different VAN-loaded NP formulations to improve the ocular delivery and corneal permeation of the drug. For this purpose, CS-NPs were developed by gelation method and characterized for physicochemical properties. Thereafter, *in vitro* release in phosphate buffer and *ex vivo* permeation through the sheep cornea were investigated. It was

expected that these systems could enhance both the drug release and permeation through the cornea.

2. Materials and Methods

2.1. Materials

Vancomycin hydrochloride (VAN) was kindly given by Exir (Lorestan, Iran). Additionally, low molecular weight chitosan hydrochloride (CS), phosphoric acid, and triethylamine were purchased from Sigma (Germany). Sodium tripolyphosphate (TPP), potassium dihydrogen phosphate, acetic acid, sodium acetate, and acetonitrile were also purchased from Merck (Germany). As well, Tryptone soya agar (TSA) and Sodium Dihydrogen Phosphate Dodecahydrate were obtained from Merck (Germany). All used chemicals were of analytical grade.

2.2. Methods

2.2.1. Preparation of Nanoparticles

The modified ionic gelation method described by Calvo et al. was adopted for the preparation of NPs in this study.[24] Three different concentrations of CS solution were prepared by addition of 150, 300, and 500 mg of CS to 50 mL of acetic acid aqueous solution (1% v/v). Thereafter, six solutions were prepared by dissolving 100 and 200 mg of VAN in each prepared CS solution. After the addition of the drug, acetic acid was added to each solution up to a total volume of 100 mL, then the solutions were magnetically stirred for 30 min at room temperature until obtaining clear solutions. Finally, the solutions were filtered by a 45 µm filter to divide any impurities.

TPP aqueous solutions were prepared at 0.25, 0.5, and 0.75 mg/mL concentrations; then added to the CS/VAN solutions drop-wise under continuous stirring to develop 12 pre-formulations. Eventually, the developed NP suspensions were centrifuged (Beckmann-Coulter® optima-L-90K, USA) for 60 min at 40,000 rpm then frozen for 2 h at a temperature of -70 °C, and lyophilized using Christ freeze-dryer alpha 2-4-LSC (Martin Christ, Osterode, Germany). Accordingly, the details on the components of each pre-formulation are indexed in Table 1.

2.2.2. Mean Particle Size, Polydispersity Index (PDI), and Zeta Potential

Each pre-formulation and formulation was evaluated for mean particle size, polydispersity index, and zeta potential using a laser diffraction particle size analyzer and zeta-sizer (Malvern Instruments, Malvern, UK). The tests were performed in triplicates and an average was reported for each sample. Finally, the optimum formulations were chosen based on their particle size and size distribution.

2.2.3. Colloidal Stability

The colloidal stability of the optimized CS/TPP NPs was evaluated during the storage at room temperature (25 °C). Within 40 days the formulations were evaluated for any changes in the mean particle size, color, appearance, and sedimentation.

2.2.4. High-Performance Liquid Chromatography (HPLC)

The VAN was separated and analyzed by the HPLC method throughout the whole study using Shimadzu chromatograph (Model LC-10ADvp) and 5 µm C18 (250 mm × 4.6 mm, Alltech, USA) analytical column. The mobile phase consisted of Acetonitrile-Triethylamine (pH=3.1) with the 10:90 v/v ratio passing through the column at the flow rate of 1 mL/min. Samples were injected

manually by a Rheodyne 7725i injector, fitted with a 20 µL sample loop. The VAN peaks were detected by UV-detector (SPD-10AVp, Shimadzu) at 280 nm as the wavelength for maximum absorbance and the elution time was measured to be 2.4 min for the drug. The calibration curve was constructed for the peak area versus concentration of the standard solutions and the drug amount was estimated by the regression equation in the further studies.

2.2.5. Loading Capacity (LC), Encapsulation Efficiency (EE), and Percentage Yield

The yield of the preparation process of NPs was calculated using the following equation:[25]

$$Yield\ (\%) = \frac{Weight\ of\ NPs}{Total\ Weight\ of\ Polymers\ and\ VAN} \quad \text{(Equation 1)}$$

To determine the LC and EE, a certain amount of NP formulations was suspended in an aqueous solution of acetic acid (2% v/v) for 30 min then sonicated for full degradation of NPs. The obtained solutions were centrifuged for 5 min at 3000 rpm and samples were withdrawn from the supernatant to be assayed by HPLC. The LC and EE were calculated using the following equations:[25]

$$EE\ (\%) = \frac{Amount\ of\ VAN\ Assayed\ in\ the\ Formulation}{Amount\ of\ VAN\ used\ for\ Preparation\ of\ the\ formulation} \quad \text{(Equation 2)}$$

$$LC\ (\%) = \frac{Amount\ of\ VAN\ Assayed\ in\ \ in\ the\ formulation}{Weight\ of\ NPs} \quad \text{(Equation 3)}$$

Accordingly, all tests were performed in triplicate and a mean was then reported.

2.2.6. Morphology

The surface morphology of NPs was analyzed by SEM using KYKY-EM 3200 (KYKY, China) device. The samples were initially suspended in deionized distilled water then spread on a platinum stab and coated by a thin layer of gold. The observation was carried out under the vacuum condition and at a 20 kV accelerating voltage.

2.2.7. *In Vitro* Antimicrobial Efficacy

The disk diffusion technique was utilized to evaluate the antimicrobial efficacy of the formulations. In this phase, *Staphylococcus aureus* was cultured and grown on TSA during 24 h of incubation at 36 °C. Afterward, aqueous suspensions of formulations were prepared and an aliquot (30 µL) of each was poured on a sterile paper disk. Subsequently, the inoculum of bacteria was prepared at a 0.5 McFarland concentration and was spread onto a TSA plate. Finally, the disks were placed onto the cultured plate and incubated for 24 h at 36 °C. The diameter of inhibition growth zones surrounding the disks was measured and reported.

2.2.8. Fourier-Transform Infrared (FTIR) Spectroscopy

The FTIR spectroscopy was performed on CS, VAN, TPP, VAN-loaded NPs, blank NPs, and a physical mixture of components to detect any interaction that occurred between the polymer and pharmacologically active groups of the drug. The samples were compressed with potassium bromide and the obtained disks were scanned within the range of 4000 to 400 cm^{-1} using Prestige-21 FTIR spectrometer (Shimadzu, Nakagyo-ku, Japan).

2.2.9. Thermogravimetric analysis (TGA)

The thermal stability of CS, VAN, TPP, NPs, and the physical mixture of components was analyzed using an STA-503 thermogravimetry analyzer (BAHR, Germany). TGA was performed in the range of 25 to 400 °C at a heating rate of 10°C/min under nitrogen flow of 6L/h.

2.2.10. *In Vitro* Release Study and Kinetics

To evaluate *in vitro* release of VAN from NPs, 5 mg of each lyophilized NP formulation were placed in a cellulose membrane dialysis bag (cut-off 12000, Sigma) along with 1 mL phosphate buffer (PBS) as the donor compartment then were immersed in 50 mL PBS (pH=7.4) as the receptor compartment. Correspondingly, the receptor compartment was agitated under 50 rpm stirring and 37.0 ± 0.5 °C temperature. The sampling was carried out at certain time intervals and the withdrawn aliquots were replaced with an equal amount of fresh PBS to preserve the sink condition. The samples were assayed using HPLC to estimate the amount of released VAN (n=3).

The data obtained by *in vitro* evaluation were fitted to different kinetical models of zero-order, first-order, and Higuchi's. The model that obtained the highest coefficient of determination (R^2) was considered the best-fitted kinetical model.

2.2.11. *Ex-Vivo* Permeation of Drug Through Isolated Sheep Cornea

The whole eyeballs of male sheep were collected immediately after the slaughter from the slaughterhouse. In the laboratory, the cornea was excised and washed with normal saline until became free of any adhering tissues, and then immediately were used in the *ex vivo* study (the protocol was approved by the Local Animal Ethical Committee of Kermanshah University of Medical Sciences; approval number: IR.KUMS.REC.1395.216)

A vertical diffusion cell was designed by a falcon tube as the donor component separated from the receptor with the sheep cornea. Ten milligrams of NP formulations were suspended in 2 mL of PBS (pH=7.4) then placed in the donor compartment. Accordingly, the cornea was tied to the end of the tube in a way that the external side was in contact with the NPs. The cell was immersed in 10 mL of PBS by the corneal side under gentle agitation and at 37.0 ± 0.5 °C temperature. Eventually, the samples (200 µL) were collected from the receptor media and replaced with an equal amount of fresh medium. The amount of permeated drug was analyzed by HPLC. Three setups were performed.

The apparent corneal permeability coefficient (P_{app}) was calculated by the following equation where the $\Delta Q/\Delta t$ (µg/min) stands for the slope of the steady-state part of the cumulative permeation versus time graph, A stands for the effective corneal penetration area (cm^2) and C_0 defined as the concentration of drug at the donor compartment (µg/mL).[26]

$$P_{app} = \frac{\Delta Q}{\Delta t.A.C_0} \qquad \text{(Equation 4)}$$

The lag time (t_L) is described as the x-intercept (time-intercept) of the steady phase of cumulative permeation versus the time curve. This is defined as the time required for the permeation curve to reach a steady phase.

3. Results and Discussion

3.1. Preparation, Mean Particle Size, PDI, and Zeta Potential

NPs were formed during the preparation process, due to the immediate occurrence of crosslinking between the phosphate groups of TPP and amino groups of CS.[27] The results of size analysis for

the pre-formulations are indexed in Table 1. It was observed that different parameters could affect the size distribution of NPs. The size distribution was extensively dependent on the concentration of CS and TPP. In this regard, it was found that in the lower levels of CS or TPP than those used for the preparation of P1, the NPs would not be formed. The obtained results also indicated that increasing of eighter CS or TPP concentrations led to a rise in the particle size which was also reported by many previous studies.[27-29] This enhancement was occurred due to the increased viscosity of the solution that decreased the efficiency of the gelation process.[30] The increased CS/TPP ratio also resulted in a higher particle size. Of note, at concentrations higher than 0.75 mg/mL for TPP and 5 mg/mL for CS, unwanted aggregation of nanoparticles could occur.[31]

Although the increased CS was responsible for an increased PDI, even at lower concentrations of CS, the PDI could increase due to the non-sufficient amount of TPP for crosslinking process.[28] Most of the formulations indicated a PDI ranged between 0.2 – 0.4 which can be considered suitable. Finally, on account of a better size and PDI, four pre-formulations of P3, P4, P11, and P12 were chosen as the optimum formulations, respectively named as F1, F2, F3, and F4 for further studies. Subsequently, the reproduced formulations showed a mean particle size of 200 to 340 nm with a PDI of 0.2 - 0.3.

Optimized formulations showed appropriate zeta potential within the range of +34 to +37 mV which could appropriately stabilize the NPs by electrostatic repulsion.[32] Additionally, the positively charged NPs would show higher affinity to the negatively charged cellular membrane and enhanced tendency to permeate through the cornea. It was found that an increased CS concentration could lead to a higher zeta potential while higher levels of TPP would lead to a decreased value due to neutralization of amino groups of CS. Accordingly, increased levels of both

CS and TPP would not change the zeta potential and almost similar values observed for F1 to F4.[28,29]

3.2. Colloidal Stability

No statistically significant changes ($p>0.05$) were observed in the mean particle size and PDI of the optimized formulations within 40 days of investigation. Accordingly, no changes were detected in the color and appearance of the formulations. Multiple factors could be considered responsible for this stability such as suitable zeta potential and electrostatic repulsion between the NPs.

3.3. Loading Capacity (LC), Encapsulation Efficiency (EE), and Percentage Yield

The calculated values for LC, EE, and yield of the preparation process are represented in table 2. The LC was measured to be between 8-26% for the formulations while EE varied between 5-6%. Clearly, higher values of LC and EE were obtained for decreased CS/TPP ratios. The main reason behind these decreased values was the higher viscosity of the concentrated CS solutions that avoid the VAN molecules from moving toward the CS molecular chain.[33] In a similar study, it was reported that in the fixed concentrations of TPP (1 mg/mL), increased CS concentration to values more than 3 mg/mL would drop the EE down to values below 20%. Another study reported 8-22% EE for CS/TPP NPs of ciprofloxacin hydrochloride.[34]

The yield of the process was almost similar for all formulations and varied independently of CS and TPP concentrations. A yield percentage of 24-84 was reported in a similar study.[35]

3.4. Morphology

The SEM images of lyophilized NPs revealed a spherical morphology and a uniform size as represented in Figure 1A. Aggregations that are detectable in the images was occurred during the freeze-drying process probably due to the hydrogen bonding between CS nanoparticles.[36] The particle size changed in the range of 133 to149 nm, which confirmed the results of the size analysis performed by the zeta-sizer.

3.5. *In Vitro* Antimicrobial Efficacy

Figure 1B is representing the result of antimicrobial testing. All the formulations showed antimicrobial efficacy against *Staphylococcus aureus* as a major microorganism involved in ocular infections and endophthalmitis. The mean diameter of inhibited growth zones was measured to be 27 ± 1 mm, 34 ± 1 mm, 31 ± 1 mm, and 37 ± 2 mm for the F1, F2, F3, and F4 formulations. Clearly, F2 and F4 showed higher diameters of inhibition growth zones due to the higher drug content. Also, it was found that the F2 and F4 formulations were more effective against *Staphylococcus aureus* compared to F1 and F3.

3.6. FTIR Spectroscopy

Figure 2 is representing the FTIR spectra of CS, TPP, VAN, drug-loaded NPS, blank NPS, and physical mixture of components. TPP spectrum showed four characteristic peaks at 1214, 1148, 1091, and 910 cm^{-1} respectively related to the P=O, PO_2, PO_3, and P-O-P stretching. Moreover, the FTIR spectrum of CS shows characteristic peaks at, 3433, 1654, 1597 cm^{-1} that are assigned to OH, acetyl, and NH_2 groups. The peak related to NH_2 groups is shifted to 1558 cm^{-1} with an extremely decreased intensity showing that most of the NH_2 groups are probably involved in the

crosslinking process with phosphate groups of TPP. Of note, the peak at 1226 cm^{-1} that appears in the spectrum of VAN-loaded NPs is attributed to the P=O bond stretching.[35]

The characteristic peaks of VAN appear at 3379 and 1662 cm^{-1} are related to -OH and C=O stretching and the peaks at 1589 and 1230 cm^{-1} are assigned to C=C, and a phenolic hydroxyl group. The characteristic peaks of VAN are presented in the VAN-loaded NP spectrum with a slight shift or reduction in intensities indicating that the drug was encapsulated inside the NPs.[35,37]

3.7. Thermogravimetric analysis (TGA)

The TGA thermographs of CS, VAN, NPs, and physical mixture of components are indicated in Figure 3. The thermograph of CS showed weight-loss at two levels; first at 25 °C to 120 °C (8%) corresponding to the moisture evaporation and next at 275°C to 310°C (39%) attributed to the decomposition of CS. In addition, VAN exhibited gradual weight-loss from 25 °C to 120 °C (16%) which could be due to the loss of water from the compound followed by two distinct thermogravimetric events at 212 °C to 286 °C (11%) and 314 °C to 391 °C (15%), respectively, related to characteristic endotherms of VAN.[38,39]

Three thermogravimetric events were also detectable in the TGA curve of NPS; the weight-loss at 25-120 °C (21%) was ascribed to evaporation of water and volatile components. Furthermore, the weight-loss stage detectable at 234-330 °C (46%) was related to the decomposition of NP's bonds and free VAN while the stage started at the 380 °C could be related to the decomposition of encapsulated VAN. The higher decomposition temperature of the encapsulated drug compared to the free drug proved that encapsulation of the drug in CS/TPP NPs could enhance the thermal stability.[40]

3.8. *In Vitro R*elease and Kinetics

The withdrawn samples of *in vitro* study were assayed by the HPLC method. Figure 4A is indicating the *in vitro* release profiles of VAN from different developed formulations. All formulations showed a burst release of 50-80% of their drug content in the first 5 h. Clearly, F1 showed a milder slope of the burst phase compared to the other formulations. In the next stage, the drug was released at a much slower rate than the first phase in a prolonged period of more than 20 h. Eventually within 11 h, F1, F2, F3, and F4 released 96.99 ± 5.05%, 95.63 ± 1.35%, 96.25 ± 1.44%, and 93.55 ± 1.26% of VAN. It was observed that due to the almost similar particle size of the formulations, all formulations released the drug in the same manner independent of the LC, EE, or polymer content. The results of the kinetics study suggested Higuchi as the best-fitted model for all the formulations because of the higher correlation coefficient. Accordingly, the burst phase occurred due to the released surface-loaded drug while the gradual phase was happened due to the release of the drug molecules loaded inside the NPs which was governed by the diffusion mechanism.[41,42] Table 3 is indexing the correlation coefficient obtained by fitting the release data in different kinetical models.

The same result was reported by Taghe et al. in a study that evaluated the *in* vitro release of ofloxacin from CS/TPP alginate NPs. The NPs released 80% of the drug in an extended period by Higuchi-like kinetics.[39] Another study showed a prolonged release of VAN from CS-based NPs during 5 h with the same kinetics.[35] Polyvinyl alcohol and Hydroxyethyl cellulose films impregnated with Eudragit L100 NPs containing the non-steroidal anti-inflammatory drug, ketorolac, were reported to be able to release the drug in the same manner for ocular delivery.[43] Eudragit L100 NPs that were loaded in Hydroxypropyl methylcellulose and Hydroxyethyl

cellulose films were reported to release azithromycin in a sustained release manner same as the present investigation.[44]

3.9. Ex-Vivo Permeation of Drug Through Isolated Sheep Cornea

Apparent permeability coefficient (P_{app}) and cumulative permeated drug through the sheep cornea into the PBS were measured for the formulations through the *ex vivo* study. The highest P_{app} was measured for F3 which was 21-folds higher than that of VAN solution. Moreover, the other formulations showed 10 to 17 times higher P_{app} compared to the conventional solution. Accordingly, these findings could prove that the NPs enhanced the corneal permeation of VAN through the sheep cornea (Table 4).

The cumulative percentage of permeated drug from each NP formulation and the VAN solution is demonstrated in Figure 4B. While only 7.41 ± 1.90% of VAN could permeate through the sheep cornea by the conventional solution during 40 h, F1, F2, F3, and F4 showed 46.54 ± 2.73%, 20.60 ± 0.02%, 66.39 ± 1.88%, and 53.57 ± 3.58% cumulative permeation in the same interval. The NP formulations indicated 3-4 folds higher effective permeation of VAN through the sheep cornea compared to the VAN solution for more than 40 h. It seems that the improved permeation of NPs is because of the lower particle size, higher surface-to-volume ratio,[45] and the high positive zeta potential.

It was suggested in previous studies that *ex vivo* permeation studies are suitable for the prediction of *in vivo* behavior of the delivery system. Hence, the result of this test could be generalized as the possible behavior of the developed systems in the animal or human eyes.[46] As described in previous studies, the reduction of the particle size in NPs come across with higher surface area of

the nanoparticles which could lead to adhesion of them to the epithelium in a wider area resulting in the formation of reservoirs that deliver the drug in a large scale to the corneal epithelium.[47] The adhesion rate was also impacted by the positive surface charge of nanoparticles which was unlike the negative dominant charge of corneal epithelium. However, other mechanisms and pathways could be also involved in the improved permeation of nanoparticles.

In a similar study atorvastatin-loaded, solid lipid nanoparticles showed a 2.2-folds higher P_{app} and 1.8-folds increased percentage of drug permeated through the cornea compared to the aqueous suspension of the drug.[48] Dexamethasone-loaded nano lipid carriers also indicated increased penetration and P_{app} compared to a drug suspension.[49] Liu et al. reported a higher permeation through cornea for hyaluronic-acid-modified lipid-polymer hybrid nanoparticles of moxifloxacin hydrochloride compared to the commercially manufactured product.[50]

Throughout the literature review, many recent studies were found with the aims parallel to the present study including controlled release, higher antibacterial efficacy, and enhanced corneal permeation. In a 2020 study, a drug-eluting suture was developed for ocular delivery of levofloxacin which indicated a 30-days drug release and efficacy against bacterial keratitis in rat eyes.[51] Mirzaeei et al. designed nanofibrous matrices for ocular delivery of ofloxacin indicated the sustained release of drug through 96 h and improved pharmacokinetics compared to the drug solution.[52] An enhanced *in vitro* antibacterial activity was reported by levofloxacin ocular nanospheres in another study.[53] Abruzzo et al. deigned VAN-loaded nanoparticles for ocular delivery in 2021, that indicated antibacterial efficacy and enhanced diffusion through the mucus layer of the eye.[54]

4. Conclusions

Vancomycin is an interesting glycopeptide antibiotic administrated for the treatment of methicillin-resistant *Staphylococcus aureus* infections which are common causes of endophthalmitis. This study aimed to design and develop vancomycin-loaded nanoparticles by the ionic gelation method using different ratios of chitosan and tripolyphosphate. The optimized formulations indicated spherical and uniform morphology, electrostatic and thermal stability, and acceptable loading capacity. Furthermore, a prolonged Higuchi-like release manner during 20 h was observed for all formulations, and an improved P_{app}, lag time, and permeation through the sheep cornea were achieved for the NP formulations compared to the conventional solution of the drug. These results indicated that vancomycin-loaded chitosan-TPP nanoparticles are suitable carriers for the ocular delivery of glycopeptide antibiotics. The sustained-release profile of these systems can decrease the frequency of administration thus increasing the acceptance of these forms by patients. The future planned research will be *in vivo* evaluation of the formulated nanoparticles.

Ethical Issues

The whole procedure was approved by the Ethics Committee (approval number: IR.KUMS.REC.1395.216), Kermanshah University of Medical Sciences, Kermanshah, Iran.

Conflict of Interest

There is no conflict of interest.

Acknowledgments

The authors would like to acknowledge the Research Council of Kermanshah University of Medical Sciences (Grant number: 92153) for financial support of this work. Also, faithfully thank Rahesh Daru Novin knowledge-intensive company for cooperation in providing materials and equipment.

References

1. Agrahari V, Mandal A, Agrahari V, Trinh HM, Joseph M, Ray A, et al. A comprehensive insight on ocular pharmacokinetics. Drug Deliv Transl Res 2016;6(6):735-54. doi: 10.1007/s13346-016-0339-2.

2. Tsai C-H, Wang P-Y, Lin I, Huang H, Liu G-S, Tseng C-L. Ocular drug delivery: Role of degradable polymeric nanocarriers for ophthalmic application. Int J Mol Sci 2018;19(9):2830. doi: 10.3390/ijms19092830.

3. Mainardes RM, Urban MC, Cinto PO, Khalil NM, Chaud MV, Evangelista RC, et al. Colloidal carriers for ophthalmic drug delivery. Curr Drug Targets 2005;6(3):363-71. doi: 10.2174/1389450053765914.

4. Davies NM. Biopharmaceutical considerations in topical ocular drug delivery. Clin Exp Pharmacol Physiol 2000;27(7):558-62. doi: 10.1046/j.1440-1681.2000.03288.x.

5. Kaur IP, Garg A, Singla AK, Aggarwal D. Vesicular systems in ocular drug delivery: An overview. Int J Pharm 2004;269(1):1-14. doi: 10.1016/j.ijpharm.2003.09.016.

6. Mehrandish S, Mirzaeei S. Design of novel nanoemulsion formulations for topical ocular delivery of itraconazole: Development, characterization and in vitro bioassay. Adv Pharm Bull Forthcoming 2022. doi: 10.34172/apb.2022.009

7. Mehrandish S, Mirzaeei S. A review on ocular novel drug delivery systems of antifungal drugs: Functional evaluation and comparison of conventional and novel dosage forms. Adv Pharm Bull 2021;11(1):28-38. doi: 10.34172/apb.2021.003

8. Mirzaeei S, Alizadeh M. Design and evaluation of soluble ocular insert for controlled release of chloramphenicol. J Rep Pharm Sci 2017;6(2):123-33.

9. Mirzaeei S, Berenjian K, Khazaei R. Preparation of the potential ocular inserts by electrospinning method to achieve the prolong release profile of triamcinolone acetonide. Adv Pharm Bull 2018;8(1):21-27. doi: 10.15171/apb.2018.00

10. Malhotra M, Majumdar D. Permeation through cornea. Indian J Exp Biol 2001;39(1):11-24.

11. Ban J, Zhang Y, Huang X, Deng G, Hou D, Chen Y, et al. Corneal permeation properties of a charged lipid nanoparticle carrier containing dexamethasone. Int J Nanomedicine 2017;12:1329-39. doi: 10.2147/IJN.S126199

12. Lakhani P, Patil A, Majumdar S. Recent advances in topical nano drug-delivery systems for the anterior ocular segment. Ther Deliv 2018;9(2):137-53. doi: 10.4155/tde-2017-0088

13. Agarwal P, Huang D, Thakur SS, Rupenthal ID. Nanotechnology for ocular drug delivery. Design of nanostructures for versatile therapeutic applications: Elsevier; 2018. p. 137-88. doi: 10.1016/B978-0-12-813667-6.00004-8.

14. Duxfield L, Sultana R, Wang R, Englebretsen V, Deo S, Swift S, et al. Development of gatifloxacin-loaded cationic polymeric nanoparticles for ocular drug delivery. Pharm Dev Technol 2016;21(2):172-9. doi: 10.3109/10837450.2015.1091839

15. Nagarwal RC, Kant S, Singh P, Maiti P, Pandit J. Polymeric nanoparticulate system: A potential approach for ocular drug delivery. J Control Release 2009;136(1):2-13. doi: 10.1016/j.jconrel.2008.12.018

16. Ilium L. Chitosan and its use as a pharmaceutical excipient. Pharm Res 1998;15(9):1326-31. doi: 10.1023/a:1011929016601

17. Motwani SK, Chopra S, Talegaonkar S, Kohli K, Ahmad FJ, Khar RK. Chitosan–sodium alginate nanoparticles as submicroscopic reservoirs for ocular delivery: Formulation, optimisation and in vitro characterisation. Eur J Pharm Biopharm 2008;68(3):513-25. doi: 10.1016/j.ejpb.2007.09.009

18. Naskar S, Koutsu K, Sharma S. Chitosan-based nanoparticles as drug delivery systems: A review on two decades of research. J Drug Target 2019;27(4):379-93. doi: 10.1080/1061186X.2018.1512112

19. De Campos AM, Sanchez A, Alonso MaJ. Chitosan nanoparticles: A new vehicle for the improvement of the delivery of drugs to the ocular surface. Application to cyclosporin a. Int J Pharm 2001;224(1-2):159-68. doi: 10.1016/s0378-5173(01)00760-8

20. Hanafy AF, Abdalla AM, Guda TK, Gabr KE, Royall PG, Alqurshi A. Ocular anti-inflammatory activity of prednisolone acetate loaded chitosan-deoxycholate self-assembled nanoparticles. Int J Nanomedicine 2019;14:3679-89. doi: 10.2147/IJN.S195892

21. Ludwig A. The use of mucoadhesive polymers in ocular drug delivery. Adv Drug Deliv Rev 2005;57(11):1595-639. doi: 10.1016/j.addr.2005.07.005

22. Calvo P, Vila-Jato JL, Alonso MJ. Comparative in vitro evaluation of several colloidal systems, nanoparticles, nanocapsules, and nanoemulsions, as ocular drug carriers. J Pharm Sci 1996;85(5):530-6. doi: 10.1021/js950474+

23. Milak S, Chemelli A, Glatter O, Zimmer A. Vancomycin ocular delivery systems based on glycerol monooleate reversed hexagonal and reversed cubic liquid crystalline phases. Eur J Pharm Biopharm 2019;139:279-90. doi: 10.1016/j.ejpb.2019.04.009

24. Calvo P, Remuñan-López C, Vila-Jato JL, Alonso MJ. Chitosan and chitosan/ethylene oxide-propylene oxide block copolymer nanoparticles as novel carriers for proteins and vaccines. Pharm Res 1997;14(10):1431-6. doi: 10.1023/a:1012128907225

25. Chaturvedi M, Molino Y, Sreedhar B, Khrestchatisky M, Kaczmarek L. Tissue inhibitor of matrix metalloproteinases-1 loaded poly(lactic-co-glycolic acid) nanoparticles for delivery across the blood-brain barrier. Int J Nanomedicine 2014;9:575-88. doi: 10.2147/IJN.S54750

26. Jiang G, Jia H, Qiu J, Mo Z, Wen Y, Zhang Y, et al. Plga nanoparticle platform for trans-ocular barrier to enhance drug delivery: A comparative study based on the application of oligosaccharides in the outer membrane of carriers. Int J Nanomedicine 2020;15:9373-87. doi: 10.2147/IJN.S272750

27. Gan Q, Wang T, Cochrane C, McCarron P. Modulation of surface charge, particle size and morphological properties of chitosan–tpp nanoparticles intended for gene delivery. Colloids Surf B Biointerfaces 2005;44(2-3):65-73. doi: 10.1016/j.colsurfb.2005.06.001

28. Luo Y, Zhang B, Cheng W-H, Wang Q. Preparation, characterization and evaluation of selenite-loaded chitosan/tpp nanoparticles with or without zein coating. Carbohydr Polym 2010;82(3):942-51. doi: 10.1016/j.carbpol.2010.06.029

29. Fan W, Yan W, Xu Z, Ni H. Formation mechanism of monodisperse, low molecular weight chitosan nanoparticles by ionic gelation technique. Colloids Surf B Biointerfaces 2012;90:21-7. doi: 10.1016/j.colsurfb.2011.09.042

30. Omar Zaki SS, Ibrahim MN, Katas H. Particle size affects concentration-dependent cytotoxicity of chitosan nanoparticles towards mouse hematopoietic stem cells. J Nanotechnol 2015;2015: 919658. https://doi.org/10.1155/2015/919658

31. Sreekumar S, Goycoolea FM, Moerschbacher BM, Rivera-Rodriguez GR. Parameters influencing the size of chitosan-tpp nano-and microparticles. Sci Rep 2018;8(1):4695. doi: 10.1038/s41598-018-23064-4

32. Honary S, Zahir F. Effect of zeta potential on the properties of nano-drug delivery systems-a review (part 2). Trop J Pharm Res 2013;12(2):265-73. doi: 10.4314/tjpr.v12i2.20

33. Gan Q, Wang T. Chitosan nanoparticle as protein delivery carrier—systematic examination of fabrication conditions for efficient loading and release. Colloids Surf B Biointerfaces 2007;59(1):24-34. doi: 10.1016/j.colsurfb.2007.04.009

34. Sobhani Z, Samani SM, Montaseri H, Khezri E. Nanoparticles of chitosan loaded ciprofloxacin: Fabrication and antimicrobial activity. Adv Pharm Bull 2017;7(3):427-32. doi: 10.15171/apb.2017.051

35. Cerchiara T, Abruzzo A, Di Cagno M, Bigucci F, Bauer-Brandl A, Parolin C, et al. Chitosan based micro-and nanoparticles for colon-targeted delivery of vancomycin prepared by alternative processing methods. Eur J Pharm Biopharm 2015;92:112-9. doi: 10.1016/j.ejpb.2015.03.004

36. Yokota H, Kadowaki M, Matsuura T, Imanaka H, Ishida N, Imamura K. The use of a combination of a sugar and surfactant to stabilize au nanoparticle dispersion against aggregation during freeze-drying. Langmuir 2020;36(24):6698-705. doi: 10.1021/acs.langmuir.0c00695

37. Mohamed HB, El-Shanawany SM, Hamad MA, Elsabahy M. Niosomes: A strategy toward prevention of clinically significant drug incompatibilities. Sci Rep 2017;7(1):6330. doi: 10.1038/s41598-017-06955-w

38. Fathi HA, Abdelkader A, AbdelKarim MS, Abdelaziz AA, El-Mokhtar MA, Allam A, et al. Electrospun vancomycin-loaded nanofibers for management of methicillin-resistant staphylococcus aureus-induced skin infections. Int J Pharm 2020;586:119620. doi: 10.1016/j.ijpharm.2020.119620

39. Taghe S, Mirzaeei S. Preparation and characterization of novel, mucoadhesive ofloxacin nanoparticles for ocular drug delivery. Braz J Pharm Sci 2019;55. https://doi.org/10.1590/s2175-97902019000117105

40. Woranuch S, Yoksan R. Eugenol-loaded chitosan nanoparticles: I. Thermal stability improvement of eugenol through encapsulation. Carbohydr Polym 2013;96(2):578-85. doi: 10.1016/j.carbpol.2012.08.117

41. Ibrahim MM, Abd-Elgawad A-EH, Soliman OA-E, Jablonski MM. Pharmaceutical nanotechnology nanoparticle-based topical ophthalmic formulations for sustained celecoxib release. J Pharm Sci 2013;102(3):1036-53. doi: 10.1002/jps.23417

42. Venkateswarlu V, Manjunath K. Preparation, characterization and in vitro release kinetics of clozapine solid lipid nanoparticles. J Control Release 2004;95(3):627-38. doi: 10.1016/j.jconrel.2004.01.005

43. Mohammadi G, Mirzaeei S, Taghe S, Mohammadi P. Preparation and evaluation of eudragit® l100 nanoparticles loaded impregnated with kt tromethamine loaded pva-hec insertions for ophthalmic drug delivery. Adv Pharm Bull 2019;9(4):593. doi: 10.15171/apb.2019.068

44. Taghe S, Mirzaeei S, Alany RG, Nokhodchi A. Polymeric inserts containing eudragit® l100 nanoparticle for improved ocular delivery of azithromycin. Biomedicines 2020;8(11):466. doi: 10.3390/biomedicines8110466

45. Schoeller J, Itel F, Wuertz-Kozak K, Gaiser S, Luisier N, Hegemann D, et al. Ph-responsive chitosan/alginate polyelectrolyte complexes on electrospun plga nanofibers for controlled drug release. Nanomaterials (Basel) 2021;11(7):1850. doi: 10.3390/nano11071850

46. Abdelbary AA, Abd-Elsalam WH, Al-Mahallawi AM. Fabrication of novel ultradeformable bilosomes for enhanced ocular delivery of terconazole: In vitro characterization, ex vivo permeation and in vivo safety assessment. Int J Pharm 2016;513(1-2):688-96. doi: 10.1016/j.ijpharm.2016.10.006

47. Muchtar S, Abdulrazik M, Frucht-Pery J, Benita S. Ex-vivo permeation study of indomethacin from a submicron emulsion through albino rabbit cornea. J Control Release 1997;44(1):55-64. doi: 10.1016/S0168-3659(96)01503-9

48. Yadav M, Schiavone N, Guzman-Aranguez A, Giansanti F, Papucci L, de Lara MJP, et al. Atorvastatin-loaded solid lipid nanoparticles as eye drops: Proposed treatment option for age-related macular degeneration (amd). Drug Deliv Transl Res 2020;10(4):919-44. doi: 10.1007/s13346-020-00733-4

49. Kiss EL, Berkó S, Gácsi A, Kovács A, Katona G, Soós J, et al. Development and characterization of potential ocular mucoadhesive nano lipid carriers using full factorial design. Pharmaceutics 2020;12(7):682. doi: 10.3390/pharmaceutics12070682

50. Liu D, Lian Y, Fang Q, Liu L, Zhang J, Li J. Hyaluronic-acid-modified lipid-polymer hybrid nanoparticles as an efficient ocular delivery platform for moxifloxacin hydrochloride. Int J Biol Macromol 2018;116:1026-36. doi: 10.1016/j.ijbiomac.2018.05.113

51. Parikh KS, Omiadze R, Josyula A, Shi R, Anders NM, He P, et al. Ultra- thin, high strength, antibiotic- eluting sutures for prevention of ophthalmic infection. Bioeng Transl Med 2021;6(2):e10204. doi: 10.1002/btm2.10204

52. Mirzaeei S, Taghe S, Asare-Addo K, Nokhodchi A. Polyvinyl alcohol/chitosan single-layered and polyvinyl alcohol/chitosan/eudragit rl100 multi-layered electrospun nanofibers as an ocular matrix for the controlled release of ofloxacin: An in vitro and in vivo evaluation. AAPS PharmSciTech 2021;22(5):170. doi: 10.1208/s12249-021-02051-5

53. De Gaetano F, Marino A, Marchetta A, Bongiorno C, Zagami R, Cristiano MC, et al. Development of chitosan/cyclodextrin nanospheres for levofloxacin ocular delivery. Pharmaceutics 2021;13(8):1293. doi: 10.3390/pharmaceutics13081293

54. Abruzzo A, Giordani B, Miti A, Vitali B, Zuccheri G, Cerchiara T, et al. Mucoadhesive and mucopenetrating chitosan nanoparticles for glycopeptide antibiotic administration. Int J Pharm 2021;606:120874. doi: 10.1016/j.ijpharm.2021.120874

Tables

Table 1. The components, size, and polydispersity index measured for CS/TPP NP pre-formulations.

Pre-Formulations	VAN (mg/mL)	CS (mg/mL)	TPP (mg/mL)	CS/TPP ratio (v/v)	Size (nm)	PDI
P1	1	1.5	0.25	10:4	190 ± 32	0.451 ± 0.037
P2	2	1.5	0.25	10:4	234 ± 18	0.371 ± 0.034
P3*	**1**	**1.5**	**0.50**	**10:4**	**215 ± 25**	**0.356 ± 0.012**
P4*	**2**	**1.5**	**0.50**	**10:4**	**219 ± 31**	**0.251 ± 0.029**
P5	1	3	0.50	10:5	333 ± 24	0.411 ± 0.045
P6	2	3	0.50	10:5	315 ± 24	0.279 ± 0.049
P7	1	3	0.75	10:5	298 ± 36	0.354 ± 0.016
P8	2	3	0.75	10:5	391 ± 41	0.411 ± 0.037
P9	1	5	0.50	10:6	369 ± 29	0.405 ± 0.022
P10	2	5	0.50	10:6	381 ± 18	0.367 ± 0.030
P11*	**1**	**5**	**0.75**	**10:6**	**369 ± 23**	**0.348 ± 0.018**
P12*	**2**	**5**	**0.75**	**10:6**	**335 ± 24**	**0.311 ± 0.015**

*Four pre-formulations chosen as optimized formulations: F1 (P3), F2 (P4), F3 (P11), and F4 (P12).

Table2. Physicochemical characterization of different formulation developed. The results are expressed as mean ± SD (n = 3).

Formulation	Size (nm)	PDI	Zeta Potential (mV)	Yield (%)	LC (%)	EE (%)
F1	208 ± 14	0.274 ± 0.034	+35.4 ± 4.2	10.3 ± 1.0	19.5 ± 2.1	5.4 ± 1.0
F2	229 ± 18	0.289 ± 0.019	+34.1 ± 7.9	11.3 ± 1.1	26.6 ± 3.0	5.5 ± 1.3
F3	331 ± 23	0.305 ± 0.029	+37.7 ± 4.8	10.8 ± 0.9	8.7 ± 1.1	6.0 ± 1.4
F4	340 ± 24	0.317 ± 0.016	+37.1 ± 6.7	11.2 ± 1.2	14.7 ± 1.4	6.1 ± 1.1

Table 3. The R^2 of different fitted kinetical models for release profiles of NPs.

Formulation	Zero-order	First-order	Higuchi
F1	0.7523	0.8569	**0.9460**

F2	0.8429	0.9467	**0.9791**
F3	0.9027	0.9776	**0.9820**
F4	0.8929	0.9572	**0.9712**

Table 4. Ex vivo corneal permeability coefficients and lag times measured for CS/TPP NPs along with the VAN aqueous solution through the sheep cornea (mean ± SD).

Formulation	**$P_{app}\times10^{-8}$ (cm/s)**	**t_L (min)**
F1	6.7 ± 0.3	< 60
F2	3.9 ± 0.5	< 60
F3	8.4 ± 0.4	< 60
F4	7.0 ± 0.5	< 60
VAN aqueous solution	0.4 ± 0.3	450

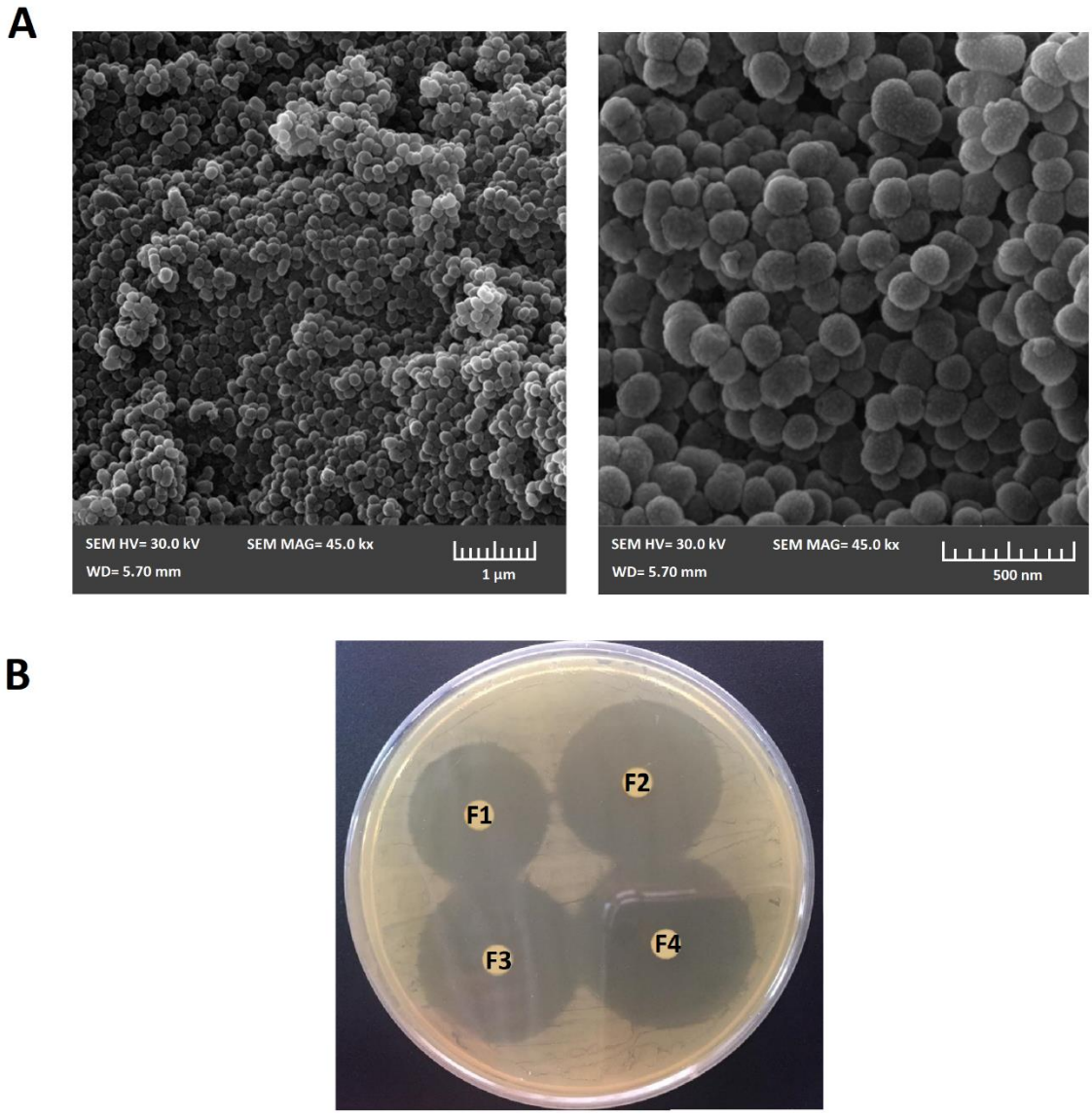

Figure 1. SEM micrograph of VAN-loaded NPs with different magnifications (A), and the result of antibacterial efficacy test of vancomycin-loaded formulations against *Staphylococcus aureus* (B).

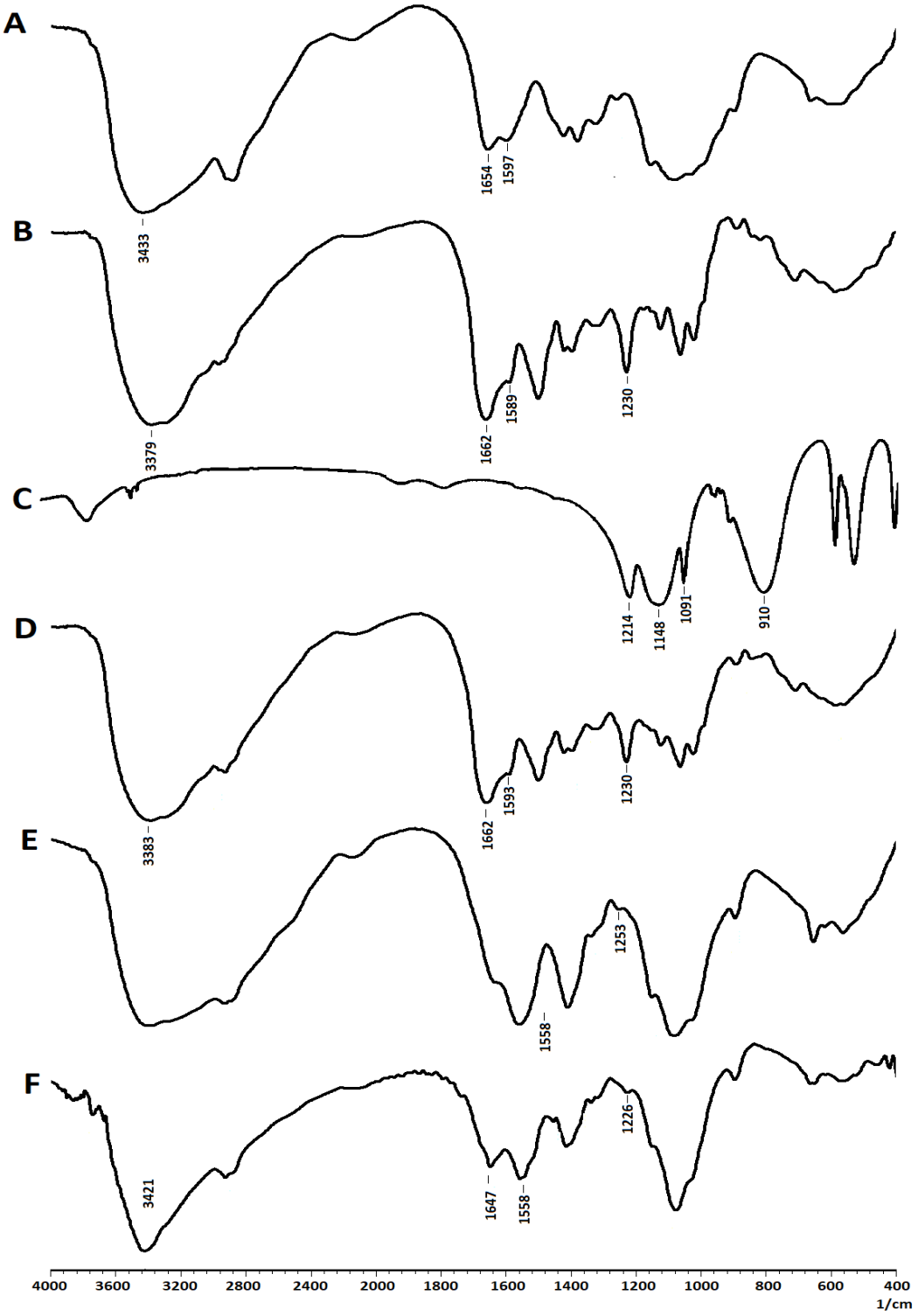

Figure 2. FTIR spectra of CS (A), VAN (B), TPP (C), physical mixture (D), blank NPs (E), and VAN-loaded NPs (F).

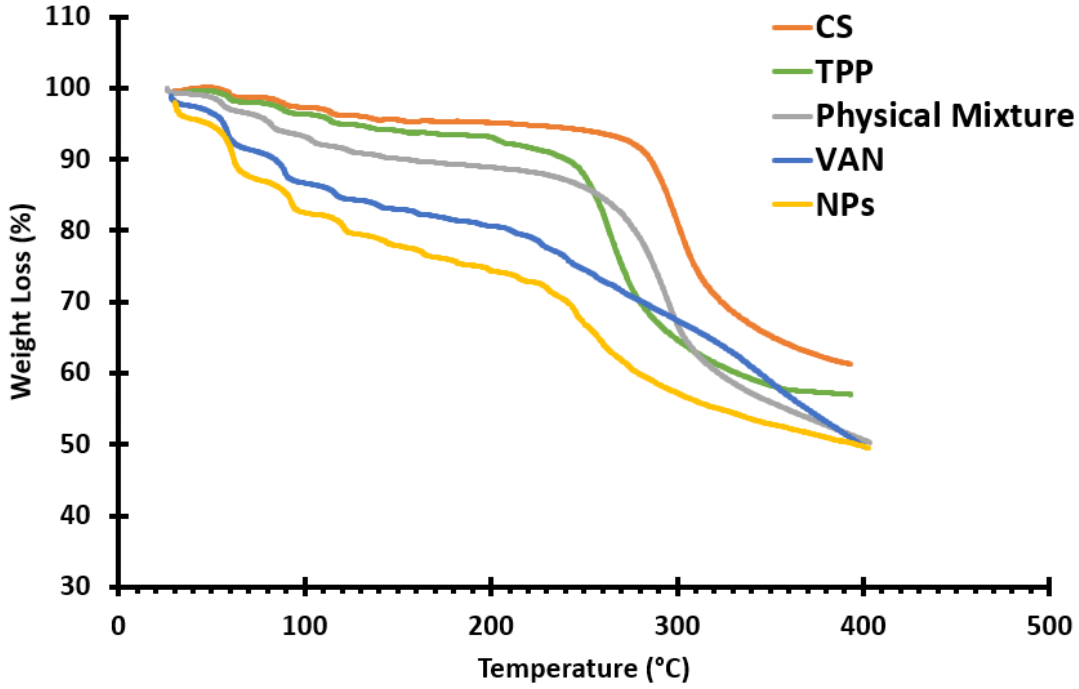

Figure 3. TGA thermogram of CS, TPP, VAN, NPs, and physical mixture of components.

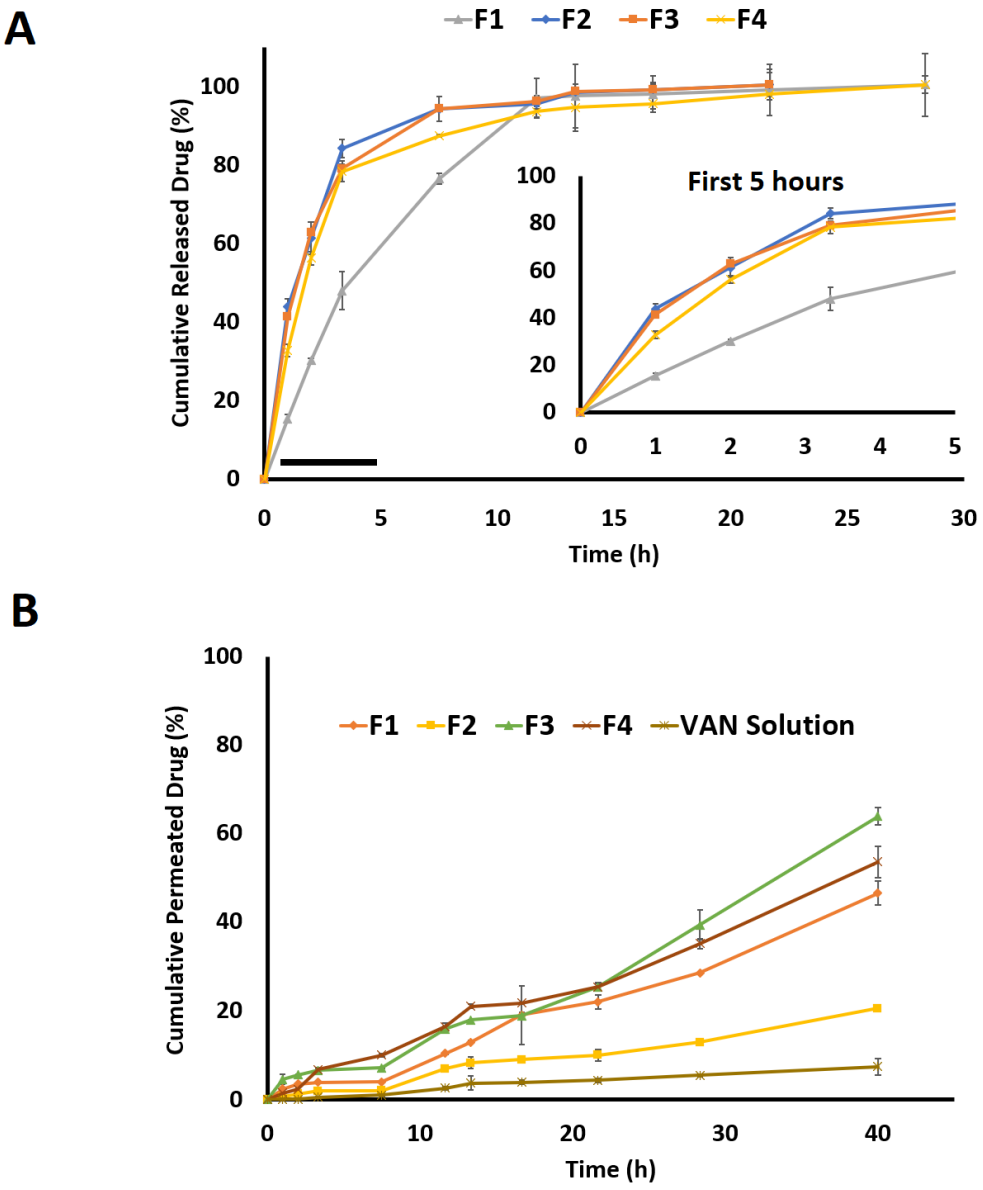

Figure 4. *In vitro* release profiles (A) of VAN from F1, F2, F3, and F4 formulations in PBS (pH=7.4). *Ex vivo* permeation of VAN from sheep cornea measured for F1, F2, F3, and F4 formulations along with VAN solution.